Dual-Mode Differential Chaos Shift Keying With Index Modulation

Xiangming Cai, Weikai Xu, *Member, IEEE*, Shaohua Hong, *Member, IEEE*, and Lin Wang, *Senior Member, IEEE*

***Abstract*— In this paper, a dual-mode differential chaos shift keying with index modulation (DM-DCSK-IM) is proposed. In the proposed system, the bit stream is partitioned into two subblocks, where the first subblock is the mapped bits used to select the active time slot, which presents the time slot's constellation mode, and the second subblcok is the modulated bits, which are further divided into two groups and modulated by a pair of distinguishable modem-mode constellations, respectively. Unlike the recently proposed pulse-position-modulation differential chaos shift keying (PPM-DCSK), since both the active and inactive time slots are applied to convey the information bits, the data rate of the proposed system can be promoted significantly. In order to detect the active time slots and recover the mapped bits as well as modulated bits correctly, we propose an effective detection algorithm for the proposed system. Furthermore, the theoretical bit error rate (BER) expressions are derived over additive white Gaussian noise (AWGN) and multipath Rayleigh fading channels, and the simulation results validate the accuracy of our derivations. Finally, the BER performance of the proposed system is compared with the other non-coherent chaotic communication systems, and the results indicate that the proposed system can offer competitive and satisfactory BER performance.**

***Index Terms*— Chaotic communication, differential chaos shift keying, index modulation, constellation, high data rate.**

I. Introduction

CHAOTIC communication has become an excellent candidate for spread-spectrum (SS) communication as the benefit of its numerous virtues, including its capacity of high resistance to jamming or interference and more immunity against multipath fading effects [1]. As a result, the above admirable features have attracted numerous research buddies to conduct the in-depth researches in chaotic communication schemes. Enjoying the advantages of simple auto-correlation receiver (AcR), i.e., without the need of complex chaotic synchronization, differential chaos shift keying (DCSK) [2] shows particular robustness against channel distortion and multipath fading [3]. As a result, DCSK has been extensively studied in various communication scenarios, including continuous mobility communication system [4], power line communication system [5], simultaneous wireless information and power transfer system [6], and noise reduction DCSK with a variational mode decomposition - independent component analysis - wavelet packet decomposition receiver [7]. In DCSK scheme, each bit duration is equally partitioned into two consecutive time slots, where the first time slot is used to carry reference signal and the second time slot is arranged for information bearing signal. Since half of the bit duration is spent on sending the non-information-bearing reference samples [8], the data rate, energy efficiency as well as spectral efficiency are rather low, which motivate the research partners to design the new high-data-rate, low-energy-consumption and high-spectral-efficiency chaotic communication schemes.

An alternative approach for improving data rate and energy efficiency is listed as follow: instead of transmitting only one information bearing signal after the reference signal, more information bits will be sent using the same reference signal. In this vein, an enhanced DCSK scheme [9] is proposed to significantly boost the data rate and reduce the energy consumption per transmitted bit. In addition to the above method, M-ary constellation design for DCSK system is an extremely effective way to achieve high data rate and spectral efficiency. Quadrature chaos shift keying (QCSK) [10], which is considered as a high-spectral-efficiency DCSK, was proposed by Galias *et al.* Generally speaking, the QCSK system can be equivalent to two DCSK system, whose information bearing signal can carry two information bits. Therefore, QCSK system doubles the data rate while owning similar BER performance as compared with DCSK system. Yet, the improvement in data rate seems feeble in the era of high data traffic. In order to obtain higher data rate, QCSK (referred to as 4-ary DCSK) is extended into the circle-constellation-based M-ary DCSK scheme [11] which is suitable for bandwidth-limited communication system differing from conventional M-ary DCSK based on Walsh codes [12]. However, it is a pity that the BER performance of the circle-constellation-based M-ary DCSK deteriorates gradually when the modulation order increases. In other words, a remarkable conclusion here is that there is a trade-off between the BER performance and data rate.

Manuscript received December 15, 2018; revised February 22, 2019 and April 7, 2019; accepted May 16, 2019. Date of publication May 23, 2019; date of current version September 16, 2019. This work was supported by the National Natural Science Foundation of China under Grant No. 61671395 and 61871337 and Guangdong Natural Science Foundation of Grant No. 2028A030313710. The associate editor coordinating the review of this paper and approving it for publication was L. Dai. *(Corresponding author: Weikai Xu.)*

X. Cai, W. Xu, and L. Wang are with the Department of Information and Communication Engineering, Xiamen University, Xiamen 361005, China (e-mail: samson0102@qq.com; xweikai@xmu.edu.cn; wanglin@xmu.edu.cn).

S. Hong is with the Department of Information and Communication Engineering, Xiamen University 361005, Xiamen, China, and also with the Shenzhen Research Institute of Xiamen University, Shenzhen 518000, China (e-mail: hongsh@xmu.edu.cn).

Color versions of one or more of the figures in this article are available online at http://ieeexplore.ieee.org.

Digital Object Identifier 10.1109/TCOMM.2019.2918518

As is well-known, the exponentially growing demand of data traffic has triggered continuous expansion in the field of wireless communication which shows no sign of being abated. Therefore, this situation encourages the wireless researchers and engineers to shift their focus to high-data-rate-oriented system design. In this vein, index modulation (IM) was born under this background. IM techniques, which consider innovative ways to convey information compared to traditional communication systems, appear as competitive candidates for next generation wireless networks due to the attractive advantages they offer in terms of spectral and energy efficiency as well as hardware simplicity [13]. In addition, IM system can provide completely new dimensions for conveying data transmission by shifting the on/off status of different transmission entities including transmitting antennas, spreading codes, subcarriers, time slots, modulation types and so on.

As a type of IM, code index modulation (CIM) was first proposed by Kaddoum *et al.* and the CIM techniques are applied to direct-sequence spread-spectrum (DSSS) system, aiming at increasing the data rate without adding extra computation complexity to the system [14], [15]. In this configuration, information bits are conveyed not only by the spread-spectrum M-ary signal constellations, but also by the activated Walsh codes which are selected by the mapped bits. The above meritorious works attract a lot of attentions and interests for the fellow researchers. For example, the authors of [16] combine the code-shifted DCSK (CS-DCSK) [17], [18] with code index modulation and propose CIM-CS-DCSK system to obtain high data rate. What a pity it is that the utilization of Walsh codes is fairly low which results in the obstacle of obtaining higher data rate. In order to manipulate this drawback, code index modulation is applied to multilevel code-shifted DCSK (MCS-DCSK) [19] and a code index modulated multilevel code-shifted DCSK (CIM-MCS-DCSK) was proposed in [20]. In this system, although the data rate is further increased, this improvement is at the expense of higher system complexity which is due to the fact that the receiver introduces more delay elements.

More recently, Xu *et al.* make a powerful combination between short reference DCSK (SR-DCSK) [21] and CIM, then propose a new non-coherent chaotic communication system, namely CIM-DCSK [22]. Compared to conventional DCSK system, the CIM-DCSK system further improves the data rate and two additional enhancement techniques are elaborated which make great progress in pursuit of excellent BER performance. Besides, some research attempts have been devoted to investigating chaotic-sequence-based index modulation. In [23], commutation code index DCSK (CCI-DCSK) is reported where additional bits are mapped into the indices of different commutation codes which are performed on reference signal for the sake of forming their orthogonal versions. Unlike the manipulation of CCI-DCSK, permutation index DCSK (PI-DCSK) [24] uses the different permuted chaotic sequences to carry additional mapped bits, which brings the benefits of high data rate and data security. Moreover, PI-DCSK system has the advantage of multiple access (MA), which is attributed to the abundant permutation set.

Since the indices of spreading codes can be used to transmit information bits by an on/off keying mechanism, IM-based chaotic communication systems have the capacity to save transmission energy from the inactive spreading codes to the active ones, which can offer preferable BER performance as compared to conventional chaotic communication systems. Recent researches have shown that the IM techniques can be applied to multi-carrier DCSK (MC-DCSK) [25]. Cheng *et al.* present two meritorious chaotic communication systems, i.e., carrier index DCSK (CI-DCSK) [26] and its M-ary version (CI-MDCSK) [27]. In both systems, the information bits are conveyed not only by DCSK as in classical MC-DCSK, but also by the indices of the subcarriers. Since a certain proportion of bits are mapped into specific subcarrier indices, which are determined by whether the subcarriers are active or not, the energy efficiency of CI-DCSK or CI-MDCSK are boosted. Additionally, in [28], the authors propose a two layer carrier index differential chaos shift keying modulation system where the modulated bits are transmitted by chaotic signals and their Hilbert transforms in specific subcarriers which are determined by two groups of index bits.

In order to further improve the BER performance of conventional M-ary DCSK, a hybrid modulation scheme based on pulse position modulation (PPM) and DCSK called PPM-DCSK is presented in [29]. Radically, PPM-DCSK system is a type of IM-based chaotic communication system. In this configuration, the positions of different time slots can be served as a dimension for data transmission. Since additional information bits are mapped into the specific indices of the active time slots, more bits can be transmitted within a symbol under the condition of same transmitted energy and thus the superior BER performance turns available. However, the utilization of time slots is quite low in PPM-DCSK system, i.e., a mass of time slots are deactivated and do not convey any information bits which results in rather low data rate and brings unnecessary loss of spectrum resources.

Although IM techniques can create complete new dimensions for data transmission in chaotic communication system, which means extra information bits can be transmitted, the throughput loss due to the waste of inactive entities is a critical problem. For example, in the recently proposed PPM-DCSK system, a mass of inactive time slots never convey any information bits, which results in the throughput loss. In order to settle this obstacle of throughput loss and further elevate the data rate, a new dual-mode differential chaos shift keying with index modulation (DM-DCSK-IM) is proposed in this paper, where the active and inactive time slots are modulated by a pair of distinguished modem-mode constellations. Meantime, the information bits are also conveyed by the specific indices of two types of time slots which are determined by the mapped bits. The main contributions of this paper are summarized as follows:

- A dual-mode differential chaos shift keying with index modulation is proposed, where the modulated bits are divided into two groups and modulated by a pair of distinguishable modem-mode constellations, respectively. Compared with the recently proposed PPM-DCSK system, the proposed DM-DCSK-IM system takes full

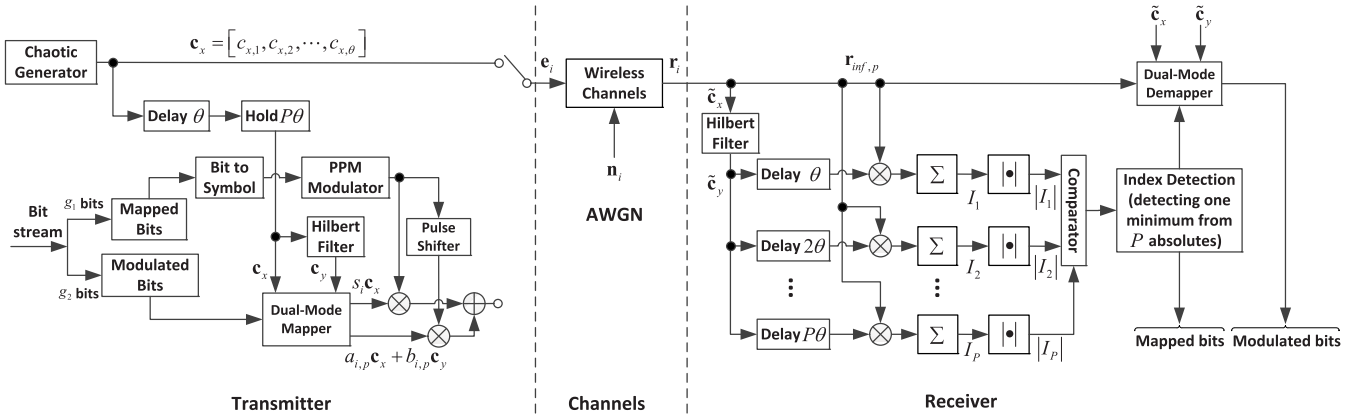

Fig. 1. The block diagram of DM-DCSK-IM system.

advantages of the idle inactive time slots to transmit information bits, which elevates the data rate significantly.
- In order to detect the active time slots and retrieve the mapped bits as well as modulated bits correctly, we propose an effective detection algorithm for the proposed DM-DCSK-IM system.
- The theoretical BER expressions of the proposed system are derived in an exhaustive manner over both AWGN and multipath Rayleigh fading channels. Then, the simulation results verify the accuracy of our derivations.
- In addition, we make a BER performance comparison between the proposed system and other non-coherent chaotic communication systems. A readily visible conclusion lies in that the proposed DM-DCSK-IM system possesses the competitive and satisfactory BER performance in contrast to its rivals.

The remainder of this paper is organized as follows. Section II describes the system model of the proposed DM-DCSK-IM in detail. System analysis of DM-DCSK-IM is arranged in Section III. Performance analysis of DM-DCSK-IM system is given in Section IV, while the numerical results and discussions are provided in Section V. Finally, our conclusions are presented in Section VI.

II. System Model

A. The Transmitter

The block diagram of DM-DCSK-IM system is depicted in Fig. 1. For the transmission of each DM-DCSK-IM symbol, the total data bits are first divided into two subblcoks, where the first subblcok of g_1 bits are provided for mapped bits and then the second subblcok of g_2 bits are arranged for modulated bits. In contrast to the existing IM-based DCSK scheme, such as PPM-DCSK, whereby merely one time slot is actively modulated and the remaining time slots keep silent, namely there are no data bits transmitted in those silent time slots. In the proposed system, all time slots including active and inactive time slots are used for transmitting data bits, which results in an enhanced data rate and spectral efficiency. The mapped bits are converted into symbol and put into the PPM modulator to map the PPM position, namely selecting an active time slot. The modulated bits are loaded into the dual-mode mapper having the constellations ∂_A and ∂_B associated with the sizes M_A and M_B, respectively, where the constellations ∂_A and ∂_B should be distinct-different, namely $\partial_A \cap \partial_B = \varnothing$. Then the modulated bits are partitioned into to two groups, where the first group bits are modulated by constellation ∂_A and the second group bits are modulated by constellation ∂_B. For example, a feasible constellation design is shown in Fig. 2. Explicitly, the DCSK and QCSK constellations are employed, where the two constellations $\partial_A = \left\{-\frac{1}{2}+0\mathrm{j}, \frac{1}{2}+0\mathrm{j}\right\}$ and $\partial_B = \left\{-\frac{\sqrt{2}}{2}+\frac{\sqrt{2}}{2}\mathrm{j}, -\frac{\sqrt{2}}{2}-\frac{\sqrt{2}}{2}\mathrm{j}, \frac{\sqrt{2}}{2}+\frac{\sqrt{2}}{2}\mathrm{j}, \frac{\sqrt{2}}{2}-\frac{\sqrt{2}}{2}\mathrm{j}\right\}$ are defined for DCSK constellation and QCSK constellation, respectively. Therefore, the transmitted signal $\mathbf{e}_i$ corresponding to i^{th} DM-DCSK-IM symbol can be given as (1), as shown at the bottom of this page.

In equation (1), $\mathbf{c}_x = [c_{x,1}, c_{x,2}, \cdots, c_{x,\theta}]$ denotes a θ-length chaotic sequence and its orthogonal chaotic sequence is $\mathbf{c}_y$, which is constructed by Hilbert filter, namely $\mathbf{c}_y = \mathcal{H}(\mathbf{c}_x)$, where $\mathcal{H}(\cdot)$ is Hilbert transform operator. $s_i = \left\{-\frac{1}{2}, \frac{1}{2}\right\}$ denotes the DCSK constellation symbol and $\otimes$ is Kronecker product operator. In addition, $a_{i,p}$ and $b_{i,p}$ are the real part and imaginary part of the p^{th} QCSK constellation symbol within the i^{th} transmitted symbol, as shown in Fig. 2. $\mathbf{S}_{PPM}^{(u_t)} = [0, 0, \cdots, 1_{u_t}, \cdots, 0]_{1\times P}$ $(P = 2^{g_1})$ is the PPM

$$\mathbf{e}_i = \left[\underbrace{\mathbf{c}_x}_{reference}, \underbrace{\mathbf{S}_{PPM}^{(u_t)} \otimes s_i\mathbf{c}_x + \sum_{p=1, p\neq u_t}^{P} \mathbf{S}_{PPM}^{(p)} \otimes (a_{i,p}\mathbf{c}_x + b_{i,p}\mathbf{c}_y)}_{information-bearing} \right]. \quad (1)$$

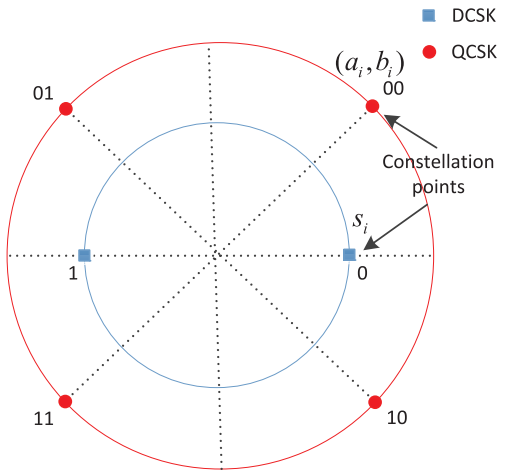

Fig. 2. An example of DM-DCSK-IM dual-mode constellation design for ∂_A and ∂_B with $M_A = 2$ and $M_B = 4$, respectively.

signal, where 1_{u_t} represents that the ${u_t}^{th}$ position of $\mathbf{S}_{PPM}^{(u_t)}$ is 1 and P denotes the total number of the time slots within the information bearing signal. Explicitly, subscript u_t represents a position index which is determined by the mapped bits. Similarly, $\mathbf{S}_{PPM}^{(p)} = [0, \cdots, 1_p, \cdots, 0, 0]_{1\times P}$, where $p = 1, 2, \cdots, P$ and $p \neq u_t$, denotes another PPM signal, which is constructed by the pulse shifter and 1_p represents that the p^{th} position of $\mathbf{S}_{PPM}^{(p)}$ is 1. In general, we define the spreading factor of the proposed DM-DCSK-IM system as $\beta = (1 + P)\,\theta$.

B. The Receiver

Assuming that the transmitted signal is contaminated by the multipath fading and additive white Gaussian noise, the received baseband discrete signal can be expressed as

$$\mathbf{r}_i = \sum_{l=1}^{L} \alpha_{i,l} \mathbf{e}_{i-\tau_{i,l}} + \mathbf{n}_i, \tag{2}$$

where L is the number of path, $\alpha_{i,l}$ and $\tau_{i,l}$ are the channel coefficient and the path delay of the l^{th} path, respectively. Then, $\mathbf{n}_i$ denotes the wideband additive white Gaussian noise vector with zero mean and covariance $\frac{N_0}{2}\mathbf{I}$, where $\mathbf{I}$ is an identity matrix. Note that when the channel parameters satisfy $L = 1$, a unit channel coefficient $\alpha_{i,1} = 1$ and zero time delay $\tau_{i,1} = 0$, the channel degrades into the case of AWGN channel. For the sake of brevity, the subscript i will be omitted in the following analysis. At the receiver, the received baseband discrete signal can be represented in a vector form with a row and $(1 + P)\,\theta$ columns given as $\mathbf{r}_i = \left[r_1, r_2, \cdots, r_{(1+P)\theta}\right]$. To be specific, the front part of $\mathbf{r}_i$ represents the received reference signal $\tilde{\mathbf{c}}_x$ with length θ described as

$$\tilde{\mathbf{c}}_x = \left[r_1, r_2, \cdots, r_\theta\right]. \tag{3}$$

Similarly, the latter part of $\mathbf{r}_i$ denotes the p^{th} information bearing signal stated as

$$\mathbf{r}_{inf,p} = \left[r_{p\theta+1}, r_{p\theta+2}, \cdots, r_{(p+1)\theta}\right], \quad p = 1, 2, \cdots, P. \tag{4}$$

TABLE I

DETECTION ALGORITHM FOR RECOVERING MAPPED BITS AND MODULATED BITS

Initialization
1) Extract the reference signal $\tilde{\mathbf{c}}_x$ and p^{th} information bearing signal $\mathbf{r}_{inf,p}$ from the received signal $\mathbf{r}_i$.
2) Load $\tilde{\mathbf{c}}_x$ into Hilbert filter to generate its orthogonal signal $\tilde{\mathbf{c}}_y$, i.e., $\tilde{\mathbf{c}}_y = \mathcal{H}(\tilde{\mathbf{c}}_x)$.

Correlation
1) The signal $\tilde{\mathbf{c}}_y$ is correlated with $\mathbf{r}_{inf,p}$ to obtain the different decision variables $I_p = [\tilde{\mathbf{c}}_y]\left[\mathbf{r}_{inf,p}\right]^{\mathrm{T}}$, $p = 1, 2, \cdots, P$.

Comparison
1) Obtain P absolute values of decision variables I_p, i.e., $\{|I_1|, |I_2|, \cdots, |I_P|\}$.
2) Estimate one minimum from $\{|I_1|, |I_2|, \cdots, |I_P|\}$ and gain its index $\hat{u}_t$ by $\hat{u}_t = \arg \min_{p=1,2,\cdots,P} (|I_p|)$.

Recovery
1) Subtract 1 from $\hat{u}_t$ and convert the $\hat{u}_t - 1$ to binary number, thus mapped bits are recovered.
2) Use the estimated index symbol $\hat{u}_t$ to determine the time slot which is used to carry DCSK symbol and remaining $P - 1$ time slots are provided for carrying QCSK symbols.
3) Recover the modulated bits from the DCSK and QCSK symbols by different demodulators in dual-mode demapper.

Clearly, in order to retrieve the transmitted bits, the receiver not only needs to detect the modulated bits from the DCSK and QCSK signal, but also the index position of PPM signal. In this vein, we propose a detection algorithm to retrieve the mapped bits as well as the modulated bits, as shown in Table I. Firstly, the received reference signal $\tilde{\mathbf{c}}_x$ is loaded into the Hilbert filter to form its orthogonal signal $\tilde{\mathbf{c}}_y$. Then, the signal $\tilde{\mathbf{c}}_y$ should be correlated with each θ-length information bearing signal $\mathbf{r}_{inf,p}$ to obtain the different decision variables I_p, formulated as

$$I_p = [\tilde{\mathbf{c}}_y]\left[\mathbf{r}_{inf,p}\right]^{\mathrm{T}}, p = 1, 2, \cdots, P. \tag{5}$$

In order to determine the index symbol, the P absolutes $\{|I_1|, |I_2|, \cdots, |I_P|\}$ are compared with each other to find the minimum value, described as

$$\hat{u}_t = \arg \min_{p=1,2,\cdots,P} (|I_p|). \tag{6}$$

After estimating the index of the least absolute value of correlator's output, the receiver knows the selected time slot used to carry DCSK symbol and also knows the remaining time slots which are applied to carry different QCSK symbols. Then, the modulated bits can be retrieved by DCSK and QCSK demodulators in dual-mode demapper.

III. SYSTEM ANALYSIS

A. Data Rate Analysis and Comparison With PPM-DCSK

In order to confirm the great superiority of the proposed DM-DCSK-IM system with respect to the data rate, we analyze the data rate of the DM-DCSK-IM system and make a comparison of data rate between the proposed system and PPM-DCSK system. For a fair comparison, we define the total number of transmitted bits carried by each symbol as the data

TABLE II
COMPARISON OF THE ATTAINABLE DATA RATE BETWEEN DM-DCSK-IM AND PPM-DCSK

P	2	4	8	16	32	64
DM-DCSK-IM (R_D)	4	9	18	35	68	133
PPM-DCSK (R_P)	2	3	4	5	6	7
$R_D - R_P$	2	6	14	30	62	126

rate R. As analyzed in the previous section, all the time slots of DM-DCSK-IM symbol are used to transmit the information bits, explicitly, one active time slot out of P time slots is modulated by the DCSK constellation and the remaining $P-1$ inactive time slots are modulated by the QCSK constellations. As a consequence, the total number of the modulated bits is expressed as $g_2 = \log_2 M_A + (P-1)\log_2 M_B = 2P-1$ and the number of the mapped bits can be given as $g_1 = \log_2 P$. Ultimately, the data rate of the proposed DM-DCSK-IM system can be calculated as the sum of the number of the mapped bits and modulated bits, i.e., $R_D = g_1 + g_2$. With respect to the PPM-DCSK system, clearly, its data rate can be stated as $R_P = \log_2 P + 1$ [29].

For the convenience of readers, the comparison of the attainable data rate between the proposed DM-DCSK-IM system and PPM-DCSK system is illustrated as Table II. Clearly, although the attainable data rate of both DM-DCSK-IM and PPM-DCSK are enlarged with the increasing of P, the data rate of DM-DCSK-IM system is increasing at a much faster rate than the counterpart of PPM-DCSK system. For example, the attainable data rate of PPM-DCSK system reaches $R_P = 5$ when $P = 16$, while the proposed DM-DCSK-IM system can achieve the data rate $R_D = 35$. In this case, the data rate gap of DM-DCSK-IM over PPM-DCSK is as high as $R_D - R_P = 30$. Moreover, as the value of P increases, the data rate gap will be more conspicuous, which demonstrates the great superiority of the proposed DM-DCSK-IM system in data rate. This phenomenon is due to the fact that the inactive time slots in PPM-DCSK never carry any information bits, while DM-DCSK-IM system gets the utmost out of the idle inactive time slots to convey information bits and thus brings a huge boost in data rate. Thus, the proposed DM-DCSK-IM system can serve as a desirable alternative for high-throughput wireless communication applications.

B. Energy Efficiency Analysis and Comparison

In order to evaluate the energy consumption of the proposed DM-DCSK-IM system, we employ the energy efficiency as an evaluation index. In [24] and [25], the authors have introduced the data-energy-to-bit-energy ratio (DBR) described as

$$DBR = \frac{E_{data}}{E_b}, \tag{7}$$

where E_{data} denotes the energy of data bearing signal, while E_b is the required total energy to carry each bit. In general, according to the transmitted signal in (1) and the signal constellation as shown in Fig. 2, the transmitted bit energy

TABLE III
DBR COMPARISON OF DM-DCSK-IM SYSTEM AND OTHER NON-COHERENT CHAOTIC COMMUNICATION SYSTEMS

System	DBR
DM-DCSK-IM	$\frac{(\mathrm{g}_1+2^{\mathrm{g}_1+1}-1)(2^{\mathrm{g}_1}-\frac{3}{4})}{2^{\mathrm{g}_1}+\frac{1}{4}}$
PPM-DCSK	$\frac{g_1+1}{2}$
PI-DCSK	$\frac{g_1+1}{2}$
CCI-DCSK	$\frac{g_1+1}{2}$
CI-DCSK	$\frac{g_1+1}{2}$

E_b can be calculated as

$$E_b = \frac{\left(2^{\mathrm{g}_1}+\frac{1}{4}\right)\sum_{k=1}^{\theta} c_{x,k}^2}{\mathrm{g}_1 + 2^{\mathrm{g}_1+1} - 1}. \tag{8}$$

Furthermore, the energy of the data bearing signal E_{data} can be expressed as

$$E_{data} = \left(2^{\mathrm{g}_1} - \frac{3}{4}\right)\sum_{k=1}^{\theta} c_{x,k}^2. \tag{9}$$

Therefore, by replacing (8) and (9) into (7), the DBR of the proposed DM-DCSK-IM system can be written as

$$DBR = \frac{E_{data}}{E_b} = \frac{\left(\mathrm{g}_1 + 2^{\mathrm{g}_1+1} - 1\right)\left(2^{\mathrm{g}_1} - \frac{3}{4}\right)}{2^{\mathrm{g}_1} + \frac{1}{4}}. \tag{10}$$

By the same token, the DBR of other non-coherent chaotic communication systems can be obtained by the similar manipulations above as depicted in the following Table III. What calls for special attention is that a higher DBR value indicates a higher energy efficiency [24]. Clearly, the proposed DM-DCSK-IM system wins the championship in terms of the energy efficiency when we take the DM-DCSK-IM system and other non-coherent chaotic communication systems into comparison. One compelling reason to explain this phenomenon lies in that instead of transmitting merely single information bearing signal after the reference signal, more information bits are transmitted sharing the same reference signal in the DM-DCSK-IM system. On the other hand, additional mapped bits are transmitted without any energy consumption. According to the above analysis, the proposed DM-DCSK-IM system makes tremendous progress concerning the energy efficiency compared to its rivals.

C. Hardware Complexity and Spectral Efficiency Comparison

In this subsection, we evaluate the hardware complexity and spectral efficiency of the proposed DM-DCSK-IM system and make a comparison with other non-coherent chaotic communication systems in the case of the same number of mapped bits per transmitted symbol, and assuming that the bandwidth is equal to B in all systems. In order to make adequate comparison with respect to hardware complexity, Table IV and Table V show the elements needed to construct DM-DCSK-IM, PPM-DCSK, PI-DCSK, CCI-DCSK and CI-DCSK transmitters and receivers, respectively. As tabulated in Table IV and Table V,

TABLE IV
TRANSMITTER HARDWARE COMPLEXITY COMPARISON

System	DM-DCSK-IM	PPM-DCSK	PI-DCSK	CCI-DCSK	CI-DCSK
Adders	1	0	0	1	1
Multipliers	2	2	1	2	$2^{g_1+1}+1$
Delay units	2^{g_1}	2^{g_1}	0	0	0
Modulator	Dual-mode modulator	DCSK modulator	DCSK modulator	DCSK modulator	DCSK modulator
Other blocks	Hilbert filter, Pulse shifter, PPM modulator	PPM modulator	Permutation block, Permutation selector	Commutation block, Pulse shaping filter, Index selector	Pulse shaping filter, Index selector

TABLE V
RECEIVER HARDWARE COMPLEXITY COMPARISON

System	DM-DCSK-IM	PPM-DCSK	PI-DCSK	CCI-DCSK	CI-DCSK
Multipliers	2^{g_1}	2^{g_1}	2^{g_1}	$2^{g_1}+1$	$2^{g_1}+1$
Delay units	2^{g_1}	2^{g_1}	0	0	0
Demodulator	Dual-mode demodulator	DCSK demodulator	DCSK demodulator	DCSK demodulator	DCSK demodulator
Other blocks	Hilbert filter, Index detection	Index detection	Permutation block, Index detection	Commutation block, Matched filter, Index detection	Matched filter, Index detection

TABLE VI
SPECTRAL EFFICIENCY COMPARISON

System	Spectral efficiency
DM-DCSK-IM	$\frac{g_1+2^{g_1+1}-1}{(1+2^{g_1})\theta B}$
PPM-DCSK	$\frac{g_1+1}{(1+2^{g_1})\theta B}$
PI-DCSK	$\frac{g_1+1}{2\theta B}$
CCI-DCSK	$\frac{g_1+1}{\theta B}$
CI-DCSK	$\frac{g_1+1}{(1+2^{g_1})\theta B}$

the Hilbert filter is performed twice in DM-DCSK-IM system to realize the dual-mode modulation and demodulation compared to other non-coherent chaotic communication systems above and the expense of hardware complexity is higher than its rival systems. However, as illustrated in Table VI, there is an admirable improvement for DM-DCSK-IM system in spectral efficiency compared to PPM-DCSK system, which is owing to that more information bits are transmitted in DM-DCSK-IM symbol than PPM-DCSK. Besides, in contrast to CCI-DCSK system, the spectral efficiency of DM-DCSK-IM system falls behind, because the essence of DM-DCSK-IM system is a kind of index modulation based on time slot which means more time slots are required. Turning back to the previous subsection and combing the analysis in current subsection, we can conclude that there is a trade-off in terms of spectral efficiency, hardware complexity and energy efficiency in the proposed DM-DCSK-IM system.

IV. PERFORMANCE ANALYSIS

A. Bit Error Probability of DM-DCSK-IM

It is pretty clear that the total number of transmitted bits per DM-DCSK-IM symbol is composed of the number of mapped bits and modulated bits. Therefore, the total BER of the proposed DM-DCSK-IM system is a function of the BER of mapped bits and modulated bits. In this vein, the bit error probability of DM-DCSK-IM system can be expressed as

$$P_{sys} = \frac{g_1}{g_1+g_2}P_{map} + \frac{g_2}{g_1+g_2}P_{mod}, \tag{11}$$

where P_{map} and P_{mod} are the BER of mapped bits and the BER of modulated bits, respectively. In addition, since the error probability of mapped bits is directly determined by whether the index detection is correct or not, the bit error rate of mapped bits P_{map} can be stated as [23], [24]

$$P_{map} = \frac{2^{(g_1-1)}}{2^{g_1}-1}P_{ed}, \tag{12}$$

where P_{ed} denotes the erroneous index detection probability of DM-DCSK-IM system. In addition, explicitly, the detection of the modulated bits contains two steps: Firstly, the index symbol should be demodulated by the minimum decision variable I_n. Secondly, the information bits carried by all time slots should be demodulated by the corresponding DCSK or QCSK demodulator. Therefore, there are two different mechanisms results in the error of modulated bits. In the first case, although the index symbol detection is correct, the detection of modulated bits is wrong. Then, in the second case, there is an error in index symbol detection. As a result, the bit error probability of the modulated bits can be calculated as

$$P_{mod} = P_e\left(1-P_{ed}\right) + P_n \cdot P_{ed}, \tag{13}$$

where P_e and P_n are the error probability of the modulated bits under the condition of correct or incorrect index detection given as

$$P_e = \frac{1}{1+2\left(P-1\right)}P_{DCSK} + \frac{2\left(P-1\right)}{1+2\left(P-1\right)}P_{QCSK}, \tag{14}$$

$$P_n = \frac{3\times 0.5 + 2(P-2)P_{QCSK}}{1+2(P-1)}, \tag{15}$$

where P_{DCSK} and P_{QCSK} are the bit error rate of DCSK demodulator and QCSK demodulator in the DM-DCSK-IM system, respectively. Particularly, in (15), the first number in numerator is 3 which is due to the fact that three bits (one from DCSK and two from QCSK) will be wrongly detected with 0.5 probability if the index detection is wrong.

B. Erroneous Index Detection Probability

According to the receiver of DM-DCSK-IM system, when the index detection is correct, i.e., $p = u_t$, the decision variable I_p corresponding to the p^{th} branch can be represented as

$$\begin{aligned} I_p &= \left[\sum_{l=1}^{L}\alpha_l \mathbf{c}_{y,\tau_l} + \hat{\mathbf{n}}_r\right]\left[\sum_{l=1}^{L}\alpha_l s\mathbf{c}_{x,\tau_l} + \mathbf{n}_{inf,p}\right]^{\mathrm{T}} \\ &= \underbrace{\sum_{l=1}^{L}\alpha_l^2 s\mathbf{c}_{y,\tau_l}\mathbf{c}_{x,\tau_l}^{\mathrm{T}}}_{=0} + \hat{\mathbf{n}}_r\mathbf{n}_{inf,p}^{\mathrm{T}} \\ &\quad + \sum_{l=1}^{L}\alpha_l\left(\mathbf{c}_{y,\tau_l}\mathbf{n}_{inf,p}^{\mathrm{T}} + s\hat{\mathbf{n}}_r\mathbf{c}_{x,\tau_l}^{\mathrm{T}}\right), \end{aligned} \tag{16}$$

where $[\cdot]^{\mathrm{T}}$ denotes transpose operator and $\hat{\mathbf{n}}_r$ is the additive white Gaussian noise superimposed upon the reference signal after Hilbert transformation with the same mean and covariance of $\mathbf{n}_i$. Similarly, $\mathbf{n}_{inf,p}$ is the additive white Gaussian noise added in the p^{th} information bearing signal and its mean and covariance are the same as the counterpart of $\mathbf{n}_i$. In addition, $\mathbf{c}_{x,\tau_l}$ and $\mathbf{c}_{y,\tau_l}$ are the delayed reference sequence and its orthogonal version, respectively. Consequently, the mean and variance of decision variable I_p can be obtained as

$$\begin{aligned} \mu_1 &= \mathrm{E}\left[I_p\right] = 0, \\ \sigma_1^2 &= \mathrm{Var}\left[I_p\right] \\ &= \sum_{l=1}^{L}\alpha_l^2\left(1+\frac{1}{4}\right)\theta\mathrm{E}\left[c^2\right]\frac{N_0}{2} + \theta\frac{N_0^2}{4} \\ &= \sum_{l=1}^{L}\alpha_l^2\frac{5E_sN_0}{2\left(4P+1\right)} + \theta\frac{N_0^2}{4} \\ &= \sum_{l=1}^{L}\alpha_l^2 E_sN_0\underbrace{\left(\frac{5}{2\left(4P+1\right)} + \frac{\theta}{4\gamma_s}\right)}_{\Omega}, \end{aligned} \tag{17, 18}$$

where $\mathrm{E}[\cdot]$ and $\mathrm{Var}[\cdot]$ are the mean operator and variance operator, respectively. E_s is the symbol energy of DM-DCSK-IM, given as $E_s = \theta\left(P+\frac{1}{4}\right)\mathrm{E}\left[c^2\right]$ where $\mathrm{E}\left[c^2\right] = \mathrm{E}\left[c_{x,\tau_l}^2\right] = \mathrm{E}\left[c_{y,\tau_l}^2\right]$ represents the chip energy of chaotic sequence. Moreover, γ_s denotes the symbol signal to noise ratio (SNR), which can be given as $\gamma_s = \sum_{l=1}^{L}\alpha_l^2\frac{E_s}{N_0}$. Similarly, when the index detection is incorrect, namely $p \neq u_t$, the decision variable of the p^{th} branch can be stated as

$$\begin{aligned} I_p' &= \left[\sum_{l=1}^{L}\alpha_l\mathbf{c}_{y,\tau_l} + \hat{\mathbf{n}}_r\right]\left[\sum_{l=1}^{L}\alpha_l\left(a_p\mathbf{c}_{x,\tau_l} + b_p\mathbf{c}_{y,\tau_l}\right) + \mathbf{n}_{inf,p}\right]^{\mathrm{T}} \\ &= \underbrace{\sum_{l=1}^{L}\alpha_l^2 a_p\mathbf{c}_{y,\tau_l}\mathbf{c}_{x,\tau_l}^{\mathrm{T}}}_{=0} + \sum_{l=1}^{L}\alpha_l^2 b_p\mathbf{c}_{y,\tau_l}\mathbf{c}_{y,\tau_l}^{\mathrm{T}} + \hat{\mathbf{n}}_r\mathbf{n}_{inf,p}^{\mathrm{T}} \\ &\quad + \sum_{l=1}^{L}\alpha_l\hat{\mathbf{n}}_r\left(a_p\mathbf{c}_{x,\tau_l}^{\mathrm{T}} + b_p\mathbf{c}_{y,\tau_l}^{\mathrm{T}}\right) + \sum_{l=1}^{L}\alpha_l\mathbf{c}_{y,\tau_l}\mathbf{n}_{inf,p}^{\mathrm{T}}. \end{aligned} \tag{19}$$

Thus, the mean and variance of I_p' can be calculated as

$$\begin{aligned} \mu_2 &= \mathrm{E}\left[I_p'\right] = \sum_{l=1}^{L}\alpha_l^2\frac{\sqrt{2}}{2}\theta\mathrm{E}\left[c^2\right] \\ &= \sum_{l=1}^{L}\alpha_l^2\frac{2\sqrt{2}E_s}{4P+1} = \sqrt{\sum_{l=1}^{L}\alpha_l^2 E_sN_0}\underbrace{\left(\frac{2\sqrt{2\gamma_s}}{4P+1}\right)}_{\Delta}, \end{aligned} \tag{20}$$

$$\begin{aligned} \sigma_2^2 &= \mathrm{Var}\left[I_p'\right] = \sum_{l=1}^{L}\alpha_l^2 2\theta\mathrm{E}\left[c^2\right]\frac{N_0}{2} + \theta\frac{N_0^2}{4} \\ &= \sum_{l=1}^{L}\alpha_l^2\frac{4E_sN_0}{4P+1} + \theta\frac{N_0^2}{4} \\ &= \sum_{l=1}^{L}\alpha_l^2 E_sN_0\underbrace{\left(\frac{4}{4P+1} + \frac{\theta}{4\gamma_s}\right)}_{\kappa}. \end{aligned} \tag{21}$$

Since the decision variables I_p and I_p' are independent Gaussian variables with the means μ_1 and μ_2, and the variances σ_1^2 and σ_2^2, both random variables $|I_p|$ and $\left|I_p'\right|$ meet the folded normal distribution [30]. In this vein, the probability density function of $|I_p|$ and the cumulative distribution function of $\left|I_p'\right|$ are formulated, respectively, as

$$f_{|I_p|}(x) = \frac{2}{\sqrt{2\pi\sigma_1^2}}\exp\left(-\frac{x^2}{2\sigma_1^2}\right), \tag{22}$$

$$F_{\left|I_p'\right|}(x) = \frac{1}{2}\left[\mathrm{erf}\left(\frac{x-\mu_2}{\sqrt{2\sigma_2^2}}\right) + \mathrm{erf}\left(\frac{x+\mu_2}{\sqrt{2\sigma_2^2}}\right)\right], \tag{23}$$

where $\exp(\cdot)$ denotes the exponential function and $\mathrm{erf}(\cdot)$ is the error function given as $\mathrm{erf}(x) = \frac{2}{\sqrt{\pi}}\int_0^x e^{-t^2}\mathrm{d}t$. Generally, let $X = \min\left(\left|I_p'\right|\right)$, $n = 1, 2, \cdots, P-1$. Since the $P-1$ decision variables are independent identically distributed random variables, the cumulative distribution function of the minimum order statistic X can be written as

$$f_X(x) = 1 - \left(1 - F_{\left|I_p'\right|}(x)\right)^{P-1}. \tag{24}$$

In particular, when the absolute value of the decision variable corresponding to the only one selected time slot is larger than the minimum absolute value of the decision variables corresponding to the non-selected time slots, there will be an error occurring. Accordingly, the erroneous index detection

probability can be derived as

$$\begin{aligned}P_{ed} &= \Pr\left[|I_p| > \min\left(\left|I'_p\right|\right)\right] \\ &= \int_0^{+\infty}\left[1-\left(1-F_{\left|I'_p\right|}(x)\right)^{P-1}\right] f_{|I_p|}(x)\,\mathrm{d}x \\ &= \frac{2}{\sqrt{2\pi\sigma_1^2}}\int_0^{+\infty}\left\{1-\left(\frac{1}{2}\right)^{P-1}\left[\mathrm{erfc}\left(\frac{x-\mu_2}{\sqrt{2\sigma_2^2}}\right)\right.\right. \\ &\quad \left.\left.+\mathrm{erfc}\left(\frac{x+\mu_2}{\sqrt{2\sigma_2^2}}\right)\right]^{P-1}\right\}\exp\left(-\frac{x^2}{2\sigma_1^2}\right)\mathrm{d}x, \end{aligned} \tag{25}$$

where $\mathrm{erfc}(\cdot)$ denotes the well-known complementary error function which is expressed as $\mathrm{erfc}(x) = 1-\mathrm{erf}(x)$. Let $x = \sqrt{\sum_{l=1}^{L}\alpha_l^2 E_s N_0}\xi$ and $\mathrm{d}x = \sqrt{\sum_{l=1}^{L}\alpha_l^2 E_s N_0}\mathrm{d}\xi$, then substituting them into the above expression (25), hence the erroneous index detection probability P_{ed} can be further simplified as

$$\begin{aligned}P_{ed} = \frac{2}{\sqrt{2\pi\Omega}}\int_0^{+\infty}&\left\{1-\left(\frac{1}{2}\right)^{P-1}\left[\mathrm{erfc}\left(\frac{\xi-\Delta}{\sqrt{2\kappa}}\right)\right.\right. \\ &\left.\left.+\mathrm{erfc}\left(\frac{\xi+\Delta}{\sqrt{2\kappa}}\right)\right]^{P-1}\right\}\exp\left(-\frac{\xi^2}{2\Omega}\right)\mathrm{d}\xi, \end{aligned} \tag{26}$$

where the parameters Ω, Δ and κ can be obtained by (18), (20) and (21), respectively.

C. BERs of DCSK and QCSK Demodulators

On the premise of correct index detection, the dual-mode demapper is applied to demodulate the modulated bits. As for the case of DCSK demodulator, its corresponding decision variable I_D can be stated as

$$\begin{aligned}I_D &= \left[\sum_{l=1}^{L}\alpha_l\mathbf{c}_{x,\tau_l}+\mathbf{n}_r\right]\left[\sum_{l=1}^{L}\alpha_l s\mathbf{c}_{x,\tau_l}+\mathbf{n}_{inf,p}\right]^{\mathrm{T}} \\ &= \sum_{l=1}^{L}\alpha_l^2 s\mathbf{c}_{x,\tau_l}\mathbf{c}_{x,\tau_l}^{\mathrm{T}}+\mathbf{n}_r\mathbf{n}_{inf,p}^{\mathrm{T}} \\ &\quad +\sum_{l=1}^{L}\alpha_l\left(\mathbf{c}_{x,\tau_l}\mathbf{n}_{inf,p}^{\mathrm{T}}+s\mathbf{n}_r\mathbf{c}_{x,\tau_l}^{\mathrm{T}}\right). \end{aligned} \tag{27}$$

Therefore, the mean and variance of I_D can be calculated as

$$\mathrm{E}[I_D] = \sum_{l=1}^{L}\alpha_l^2\frac{1}{2}\theta\mathrm{E}\left[c^2\right] = \sum_{l=1}^{L}\alpha_l^2\frac{2E_s}{4P+1}, \tag{28}$$

$$\begin{aligned}\mathrm{Var}[I_D] &= \sum_{l=1}^{L}\alpha_l^2\left(1+\frac{1}{4}\right)\theta\mathrm{E}\left[c^2\right]\frac{N_0}{2}+\theta\frac{N_0^2}{4} \\ &= \sum_{l=1}^{L}\alpha_l^2\frac{5E_sN_0}{2(4P+1)}+\theta\frac{N_0^2}{4}. \end{aligned} \tag{29}$$

Similarly, regarding the QCSK demodulators, since all the $P-1$ QCSK demodulators are independent of each other and have the same error probability, we only need to evaluate the bit error probability of one of them. Therefore, the decision variables I_Q^a and I_Q^b corresponding to the in-phase component and quadrature component of QCSK demodulator can be given, respectively, as

$$\begin{aligned}&I_Q^a \\ &= \left[\sum_{l=1}^{L}\alpha_l\mathbf{c}_{x,\tau_l}+\mathbf{n}_r\right]\left[\sum_{l=1}^{L}\alpha_l\left(a_p\mathbf{c}_{x,\tau_l}+b_p\mathbf{c}_{y,\tau_l}\right)+\mathbf{n}_{inf,p}\right]^{\mathrm{T}} \\ &= \sum_{l=1}^{L}\alpha_l^2 a_p\mathbf{c}_{x,\tau_l}\mathbf{c}_{x,\tau_l}^{\mathrm{T}}+\underbrace{\sum_{l=1}^{L}\alpha_l^2 b_p\mathbf{c}_{x,\tau_l}\mathbf{c}_{y,\tau_l}^{\mathrm{T}}}_{=0}+\mathbf{n}_r\mathbf{n}_{inf,p}^{\mathrm{T}} \\ &\quad +\sum_{l=1}^{L}\alpha_l\mathbf{n}_r\left(a_p\mathbf{c}_{x,\tau_l}^{\mathrm{T}}+b_p\mathbf{c}_{y,\tau_l}^{\mathrm{T}}\right)+\sum_{l=1}^{L}\alpha_l\mathbf{c}_{x,\tau_l}\mathbf{n}_{inf,p}^{\mathrm{T}}, \end{aligned} \tag{30}$$

$$\begin{aligned}&I_Q^b \\ &= \left[\sum_{l=1}^{L}\alpha_l\mathbf{c}_{y,\tau_l}+\hat{\mathbf{n}}_r\right]\left[\sum_{l=1}^{L}\alpha_l\left(a_p\mathbf{c}_{x,\tau_l}+b_p\mathbf{c}_{y,\tau_l}\right)+\mathbf{n}_{inf,p}\right]^{\mathrm{T}} \\ &= \underbrace{\sum_{l=1}^{L}\alpha_l^2 a_p\mathbf{c}_{y,\tau_l}\mathbf{c}_{x,\tau_l}^{\mathrm{T}}}_{=0}+\sum_{l=1}^{L}\alpha_l^2 b_p\mathbf{c}_{y,\tau_l}\mathbf{c}_{y,\tau_l}^{\mathrm{T}}+\hat{\mathbf{n}}_r\mathbf{n}_{inf,p}^{\mathrm{T}} \\ &\quad +\sum_{l=1}^{L}\alpha_l\hat{\mathbf{n}}_r\left(a_p\mathbf{c}_{x,\tau_l}^{\mathrm{T}}+b_p\mathbf{c}_{y,\tau_l}^{\mathrm{T}}\right)+\sum_{l=1}^{L}\alpha_l\mathbf{c}_{y,\tau_l}\mathbf{n}_{inf,p}^{\mathrm{T}}. \end{aligned} \tag{31}$$

As a result, the means and variances of I_Q^a and I_Q^b can be deduced as

$$\mathrm{E}\left[I_Q^a\right] = \mathrm{E}\left[I_Q^b\right] = \sum_{l=1}^{L}\alpha_l^2\frac{\sqrt{2}}{2}\theta\mathrm{E}\left[c^2\right] = \sum_{l=1}^{L}\alpha_l^2\frac{2\sqrt{2}E_s}{4P+1}, \tag{32}$$

$$\begin{aligned}\mathrm{Var}\left[I_Q^a\right] &= \mathrm{Var}\left[I_Q^b\right] = \sum_{l=1}^{L}\alpha_l^2 2\theta\mathrm{E}\left[c^2\right]\frac{N_0}{2}+\theta\frac{N_0^2}{4} \\ &= \sum_{l=1}^{L}\alpha_l^2\frac{4E_sN_0}{4P+1}+\theta\frac{N_0^2}{4}. \end{aligned} \tag{33}$$

According to (28) and (29), the bit error probability of DCSK is equal to

$$\begin{aligned}P_{DCSK} &= \frac{1}{2}\mathrm{erfc}\left[\left(\frac{2\mathrm{Var}[I_D]}{\left(\mathrm{E}[I_D]\right)^2}\right)^{-\frac{1}{2}}\right] \\ &= \frac{1}{2}\mathrm{erfc}\left[\left(\frac{5(4P+1)}{4\gamma_s}+\frac{\theta(4P+1)^2}{8\gamma_s^2}\right)^{-\frac{1}{2}}\right]. \end{aligned} \tag{34}$$

Similarly, according to (32) and (33), the bit error rate of QCSK can be formulated as [10]

$$P_{QCSK} = \frac{1}{2}\mathrm{erfc}\left[\left(\frac{4P+1}{\gamma_s}+\frac{\theta(4P+1)^2}{16\gamma_s^2}\right)^{-\frac{1}{2}}\right]. \tag{35}$$

Substituting (34) and (35) into (14) and (15), the error probability P_e and P_n can be obtained. Subsequently, substituting (12) and (13) into (11), the bit error rate of DM-DCSK-IM system can be obtained. Considering the case of L independent and identically distributed (i.i.d) Rayleigh-fading

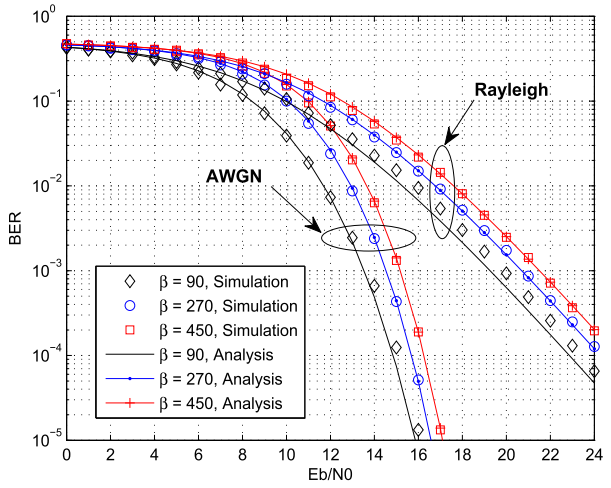

Fig. 3. BER performance of DM-DCSK-IM system over AWGN and multipath Rayleigh fading channels with $g_1 = 1$ and $\beta = 90, 270, 450$, respectively.

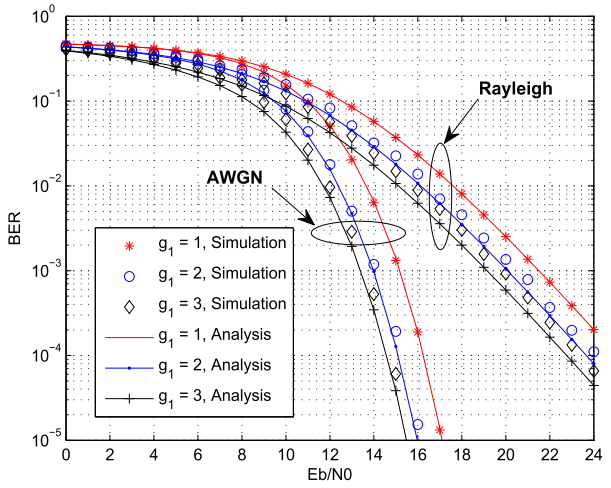

Fig. 4. BER performance of DM-DCSK-IM system over AWGN and multipath Rayleigh fading channels with $\beta = 450$ and $g_1 = 1, 2, 3$, respectively.

channels, the probability density function of the symbol-SNR γ_s can be obtain as [25], [31], [32]

$$f(\gamma_s) = \frac{\gamma_s^{L-1}}{(L-1)!\bar{\gamma}_c^L} \exp\left(-\frac{\gamma_s}{\bar{\gamma}_c}\right), \tag{36}$$

where $\bar{\gamma}_c = \frac{E_s}{N_0}\mathrm{E}\left[\alpha_j^2\right] = \frac{E_s}{N_0}\mathrm{E}\left[\alpha_l^2\right]$, $j \neq l$ denotes the average symbol-SNR per channel and $\sum_{l=1}^{L} \mathrm{E}\left[\alpha_l^2\right] = 1$. Finally, the averaged bit error rate of the DM-DCSK-IM system over multipath Rayleigh fading channel can be expressed as

$$\bar{P}_{sys} = \int_0^{\infty} P_{sys} \cdot f(\gamma_s) \mathrm{d}\gamma_s. \tag{37}$$

Note that the above expression (37) is also applicable to the case of AWGN channel when only the first path with the propagation gain $\alpha_1 = 1$ is considered.

V. Numerical Results and Discussions

In this section, Monte Carlo simulations are carried out to evaluate the BER performance of the proposed DM-DCSK-IM system with the different parameters over AWGN and multipath Rayleigh fading channels. In simulation, the chaotic sequences are generated by the second-order Chebyshev polynomial function (CPF) $x_{k+1} = 1 - 2x_k^2$ [25], [33]. For multipath Rayleigh fading channel, three paths $L = 3$ are considered, having equal average power gain, i.e., $\mathrm{E}\left[\alpha_1^2\right] = \mathrm{E}\left[\alpha_2^2\right] = \mathrm{E}\left[\alpha_3^2\right] = \frac{1}{3}$, with time delays $\tau_1 = 0$, $\tau_2 = 1$ and $\tau_3 = 2$, respectively.

A. Performance Evaluation

In order to confirm the accuracy of our theoretical derivation in the above section, the simulation results of the proposed DM-DCSK-IM system are compared with the corresponding theoretical results over AWGN and multipath Rayleigh fading channels, as shown in Fig. 3. It is clearly observed that the simulation results match the theoretical ones well for both AWGN and multipath Rayleigh fading channels, which verifies that our theoretical analysis is valid and accurate. From another perspective, as depicted in Fig. 3, the BER performance of the DM-DCSK-IM system deteriorates as the spreading factor β enlarges. The phenomenon is due to the fact that when the spreading factor is large, the contribution of noise-noise cross correlation term becomes more significant, which results in the degradation of BER performance.

In Fig. 4, we evaluate the BER performance of the DM-DCSK-IM system over AWGN and multipath Rayleigh fading channels with $\beta = 450$ and $g_1 = 1, 2, 3$, respectively. Clearly, the simulation results are in a good agreement with the corresponding theoretical results, which verifies the accuracy of our derivations. As illustrated Fig. 4, when g_1 increases, the BER performance of the proposed DM-DCSK-IM system improves. For example, in AWGN channel, DM-DCSK-IM system needs 17dB to achieve the BER level of 10^{-5} when $g_1 = 1$. By contrast, as for the case of $g_1 = 3$, the required SNR is reduced to about 15.5dB in the same BER level above. In other words, the BER performance gain is 1.5dB between $g_1 = 3$ and $g_1 = 1$. Moreover, the BER performance improvement between $g_1 = 3$ and $g_1 = 1$ is about 2dB in multipath Rayleigh fading channel. As a matter of fact, this phenomenon can be explained that with the increasing of g_1, i.e., higher proportion of mapped bits corresponding to the total bits within a symbol, there will be more energy spending on modulated bits which contributes to preferable BER performance.

To explore the influence of channel time delay τ_2 on the BER performance of the proposed DM-DCSK-IM system, we simulate the DM-DCSK-IM system in the condition of two-path Rayleigh fading channels with the equal power gains, i.e., $\mathrm{E}\left(\alpha_1^2\right) = \mathrm{E}\left(\alpha_2^2\right) = \frac{1}{2}$ and different channel time delays τ_2. As shown in Fig. 5, when the channel time delay τ_2 is quite low, the inter symbol interference can be neglected and thus the simulation results and the corresponding theoretical results match very well. However, the BER performance degradation which is derived from the inter symbol interference is rather obvious when the value of τ_2 increases. In addition, the proposed DM-DCSK-IM system with larger spreading

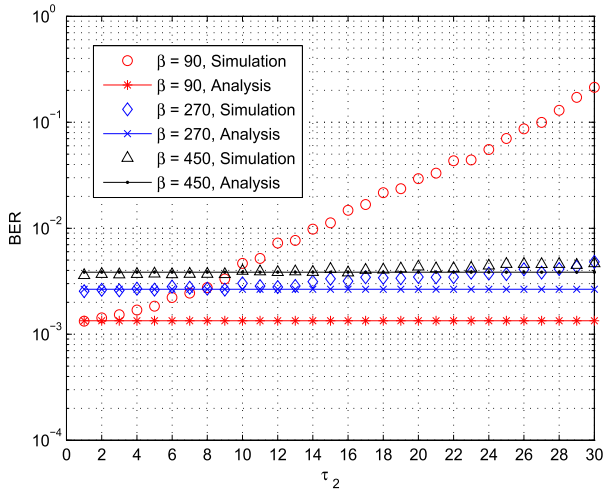

Fig. 5. The effect of channel time delay τ_2 on the BER performance of DM-DCSK-IM system over two-path Rayleigh fading channel with $\frac{E_b}{N_0} = 22$dB, $g_1 = 1$ and $\beta = 90, 270, 450$, respectively.

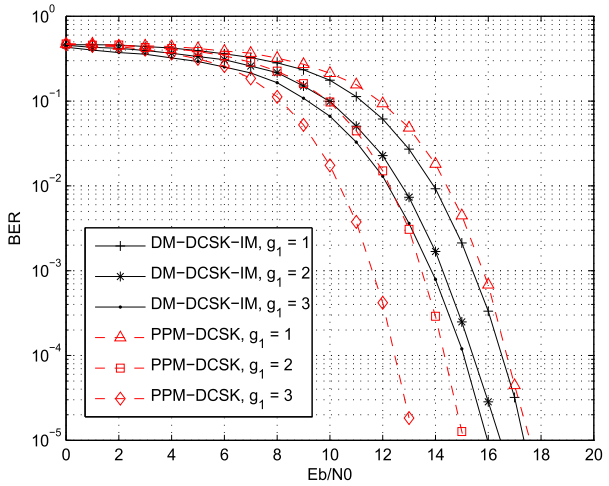

Fig. 6. BER performance comparison between DM-DCSK-IM system and PPM-DCSK system over AWGN channel with $\beta = 540$ and $g_1 = 1, 2, 3$, respectively.

factor shows stronger robustness than the smaller counterpart in the case of large channel time delay.

B. Performance Comparison

In Fig. 6, we make a BER performance comparison between the DM-DCSK-IM system and the recently proposed PPM-DCSK system over AWGN channel with $\beta = 540$ and $g_1 = 1, 2, 3$, respectively. As displayed in Fig. 6, the BER performances of both DM-DCSK-IM system and PPM-DCSK system are taking a turn for the better with the increasing of g_1. In the case of $g_1 = 1$, the BER performance of the proposed DM-DCSK-IM system outperforms the counterpart of PPM-DCSK system slightly. Furthermore, the data rate of the DM-DCSK-IM system is the double of that of PPM-DCSK system. With respect of $g_1 = 3$, PPM-DCSK system shows better BER performance than DM-DCSK-IM system and, explicitly, the BER performance gap between PPM-DCSK system and DM-DCSK-IM system is less than 2.5dB at BER level 10^{-5}. However, as clearly witnessed in Table II, it should be taken notice of that the data rate of the proposed DM-DCSK-IM system is four and a half times the counterpart of PPM-DCSK system. Therefore, there is a trade-off between DM-DCSK-IM system and PPM-DCSK system in terms of the data rate and BER performance. From another perspective, since $P-1$ idle inactive time slots never carry any information bits in PPM-DCSK system which causes a mass of waste of spectrum resources, the spectral efficiency of PPM-DCSK system is extremely low. By contrast, this drawback is solved pretty well in the proposed DM-DCSK-IM system.

In addition, the BER performance of the proposed DM-DCSK-IM system is compared with the counterpart of PPM-DCSK system over multipath Rayleigh fading channel with $\beta = 540$ and $g_1 = 1, 2, 3$, respectively. As shown in Fig. 7, explicitly, it offers DM-DCSK-IM system a BER performance superior that of PPM-DCSK system when $g_1 = 1$, which is similar to the case of AWGN channel. Under the condition of $g_1 = 2$, clearly, although the BER performance of the

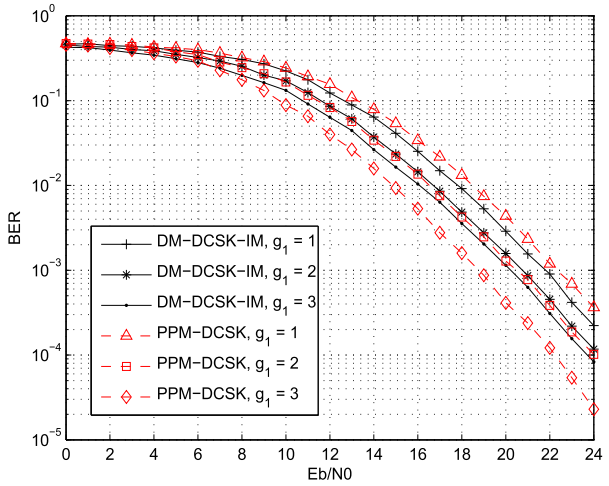

Fig. 7. BER performance comparison between DM-DCSK-IM system and PPM-DCSK system over multipath Rayleigh fading channel with $\beta = 540$ and $g_1 = 1, 2, 3$, respectively.

DM-DCSK-IM system and PPM-DCSK system is pretty similar, the DM-DCSK-IM system can achieve three times data rate in contrast to PPM-DCSK system. When the value of g_1 is relative large, such as $g_1 = 3$, the performance of DM-DCSK-IM system is worse than PPM-DCSK system. Nevertheless, the data rate of DM-DCSK-IM system has great advantage over PPM-DCSK system, as shown in Table II. In other words, the DM-DCSK-IM system is especially suitable for the high-throughput scenarios and also has the satisfactory BER performance. To be specific, the primary difference between the DM-DCSK-IM system and PPM-DCSK system lies in that the DM-DCSK-IM system takes full advantage of the inactive time slots to convey additional information bits which means there is enormous interference in the process of index detection and it results in poor BER performance.

In order to confirm the excellent BER performance of the DM-DCSK-IM system, we compare the performance of DM-DCSK-IM system and other non-coherent IM-based chaotic communication systems over AWGN and multipath

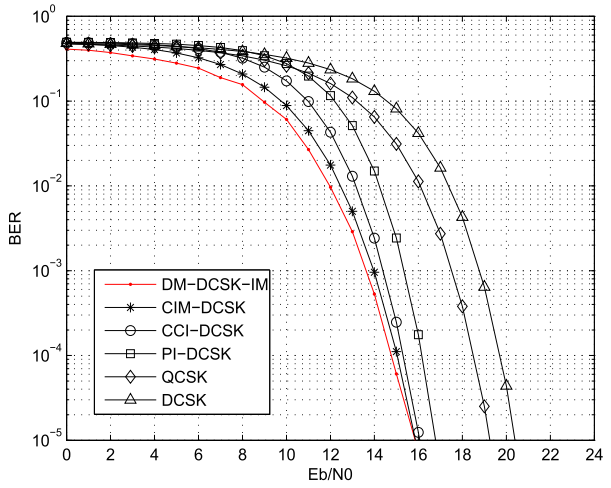

Fig. 8. BER performance comparison between DM-DCSK-IM system and other non-coherent chaotic communication systems over AWGN channel with $g_1 = 3$ and $\beta = 450$.

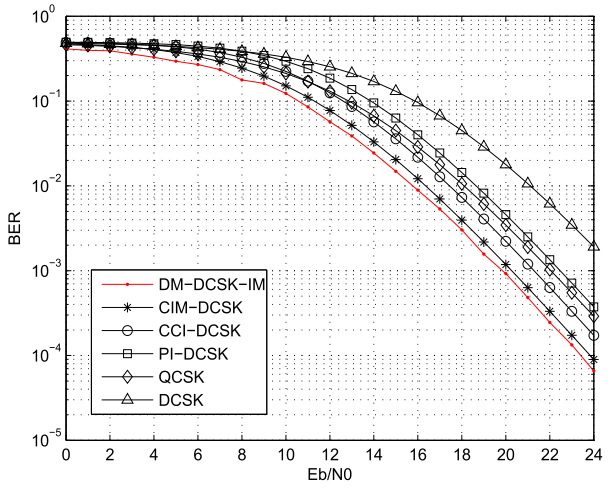

Fig. 9. BER performance comparison between DM-DCSK-IM system and other non-coherent chaotic communication systems over multipath Rayleigh fading channel with $g_1 = 3$ and $\beta = 450$.

Rayleigh fading channels, respectively. In addition, the BER performances of DCSK and QCSK systems are listed as well for reference. For the sake of fairness, the number of mapped bits and spreading factors for all systems are the same, i.e., $g_1 = 3$ and $\beta = 450$. In the case of AWGN channel, as depicted in Fig. 8, the proposed DM-DCSK-IM system achieves the best BER performance compared to other non-coherent chaotic communication systems enumerated above. More specifically, the BER performance improvement of DM-DCSK-IM system over the classical DCSK system is greater than 4dB at BER level 10^{-5}. In regard to the case of multipath Rayleigh fading channel, as clearly observed in Fig. 9, the proposed DM-DCSK-IM system shows the best BER performance among other chaotic communication systems, which verifies that DM-DCSK-IM system possesses strong robustness in the environment of noise jamming and fading propagation environment. For example, QCSK system needs 22.5dB to reach the BER level of 10^{-3}, while the required SNR of DM-DCSK-IM system is less than 20dB in the same BER level. That means the BER performance gain of the proposed DM-DCSK-IM system over QCSK system is 2.5dB at 10^{-3} BER level. Although the performance of CIM-DCSK system is quite close to the counterpart of DM-DCSK-IM system, the data rate of DM-DCSK-IM system is several times that of CIM-DCSK system.

As clearly shown in Fig. 10, we make a BER performance comparison between the proposed DM-DCSK-IM system and other non-coherent chaotic communication systems over AWGN and multipath Rayleigh fading channels with the same number of bits per symbol. In the systems listed in Fig. 10, the number of transmitted bits is set to 4 and $\beta = 360$. As illustrated, the BER performance of the proposed DM-DCSK-IM system shows worse than the counterpart of CIM-DCSK and CCI-DCSK systems. Explicitly, in AWGN channel, the CIM-DCSK system obtains about 1dB performance gain compared to DM-DCSK-IM system at the BER level 10^{-5}. Regarding to the multipath Rayleigh fading channel, the BER performance of DM-DCSK-IM and CCI-DCSK system are almost the same, while the BER performance improvement of DM-DCSK-IM

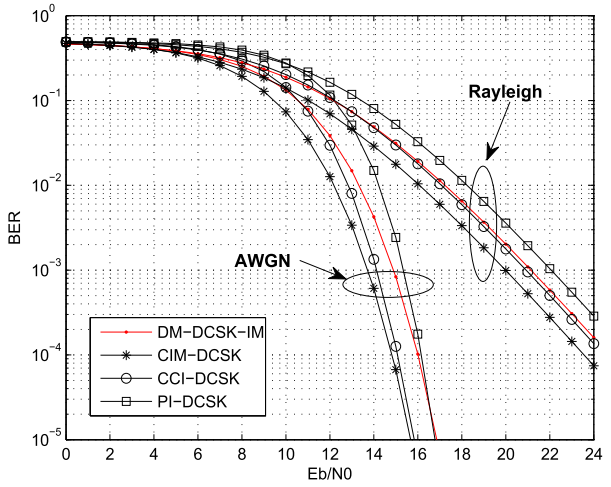

Fig. 10. BER performance comparison between DM-DCSK-IM system and other non-coherent chaotic communication systems over AWGN and multipath Rayleigh fading channels with the same number of bits per symbol and $\beta = 360$.

system over PI-DCSK system is quite close to 1dB at the BER of 10^{-3}. As a matter of fact, in order to obtain 4 bits per transmitted symbol, CIM-DCSK, CCI-DCSK and PI-DCSK systems need 3 mapped bits and 1 modulated bit, by contrast, the proposed DM-DCSK-IM system just uses 1 mapped bit and 3 modulated bits to form 4 bits per symbol which means the proportion of modulated bits in DM-DCSK-IM system is higher than its rivals, thereby causing the poor BER performance of DM-DCSK-IM system.

VI. Conclusion

In this paper, a dual-mode differential chaos shift keying with index modulation has been proposed and analyzed in an exhaustive manner. In contrast to the existing PPM-DCSK system, all the time slots, including the active time slot and idle inactive time slots, are modulated by a pair of distinguishable modem-mode constellations, respectively, in the

proposed DM-DCSK-IM system, which enhances the data rate and spectral efficiency. Moreover, the data rate, hardware complexity and spectral efficiency of DM-DCSK-IM system are compared with the recently proposed PPM-DCSK system, it is worthy to notice that the data rate of DM-DCSK-IM system greatly exceeds the counterpart of PPM-DCSK at the expend of hardware complexity. In order to detect the active time slots and retrieve the mapped bits as well as modulated bits correctly, we propose an effective detection algorithm for the proposed DM-DCSK-IM system. In addition, we have derived the theoretical expressions for DM-DCSK-IM system over AWGN and multipath Rayleigh fading channels, and the simulation results validate our theoretical derivations. Then, in order to demonstrate the excellent BER performance of DM-DCSK-IM system, we make a BER performance comparison between DM-DCSK-IM system and other non-coherent chaotic communication systems. The results have confirmed that the proposed DM-DCSK-IM system is capable of achieving a satisfactory BER performance. In a word, the proposed DM-DCSK-IM system has the competitive and satisfactory BER performance and data rate compared to its rivals. Our future works will focus on IM-based DCSK system using multiple-mode constellations, where multiple distinguishable constellations are employed to convey information bits. Besides, we will also investigate the optimization of the constellation design of DM-DCSK-IM system to further improve the BER performance.

REFERENCES

[1] M. Sushchik, L. S. Tsimring, and A. R. Volkovskii, "Performance analysis of correlation-based communication schemes utilizing chaos," *IEEE Trans. Circuits Syst. I, Fundam. Theory Appl.*, vol. 47, no. 12, pp. 1684–1691, Dec. 2000.

[2] G. Kolumbán, B. Vizvári, W. Schwarz, and A. Abel, "Differential chaos shift keying: A robust coding for chaos communication," in *Proc. Nonlinear Dyn. Electron. Syst*, Seville, Spain, Jun. 1996, pp. 87–92.

[3] M. Dawa, G. Kaddoum, and Z. Sattar, "A generalized lower bound on the bit error rate of DCSK systems over multi-path Rayleigh fading channels," *IEEE Trans. Circuits Syst., II, Exp. Briefs*, vol. 65, no. 3, pp. 321–325, Mar. 2018.

[4] F. J. Escribano, G. Kaddoum, A. Wagemakers, and P. Giard, "Design of a new differential chaos-shift-keying system for continuous mobility," *IEEE Trans. Commun.*, vol. 64, no. 5, pp. 2066–2078, May 2016.

[5] G. Kaddoum and N. Tadayon, "Differential chaos shift keying: A robust modulation scheme for power-line communications," *IEEE Trans. Circuits Syst., II, Exp. Briefs*, vol. 64, no. 1, pp. 31–35, Jan. 2017.

[6] G. Kaddoum, H.-V. Tran, L. Kong, and M. Atallah, "Design of simultaneous wireless information and power transfer scheme for short reference DCSK communication systems," *IEEE Trans. Commun.*, vol. 65, no. 1, pp. 431–443, Jan. 2017.

[7] B. Van Nguyen, M. T. Nguyen, H. Jung, and K. Kim, "Designing anti-jamming receivers for NR-DCSK systems utilizing ICA, WPD, and VMD methods," *IEEE Trans. Circuits Syst., II, Exp. Briefs*, to be published. doi: 10.1109/TCSII.2019.2891254.

[8] F. C. M. Lau and C. K. Tse, *Chaos-Based Digital Communication Systems: Operating Principles, Analysis Methods, and Performance Evaluation*. Berlin, Germany: Springer-Verlag, 2003.

[9] G. Kolumban, Z. Jako, and M. P. Kennedy, "Enhanced versions of DCSK and FM-DCSK data transmission systems," in *Proc. 1999 IEEE Int. Symp. Circuits Syst. VLSI*, Orlando, FL, USA, May/Jun. 1999, pp. 475–478.

[10] Z. Galias and G. M. Maggio, "Quadrature chaos-shift keying: Theory and performance analysis," *IEEE Trans. Circuits Syst. I, Reg. Papers*, vol. 48, no. 12, pp. 1510–1519, Dec. 2001.

[11] L. Wang, G. Cai, and G. R. Chen, "Design and performance analysis of a new multiresolution M-ary differential chaos shift keying communication system," *IEEE Trans. Wireless Commun.*, vol. 14, no. 9, pp. 5197–5208, Sep. 2015.

[12] G. Kis, "Performance analysis of chaotic communication systems," Ph.D. dissertation, Dept. Meas. Inf. Syst., Budapest Univ. Technol. Econ., Budapest, Hungary, 2005.

[13] E. Basar, M. Wen, R. Mesleh, M. Di Renzo, Y. Xiao, and H. Haas, "Index modulation techniques for next-generation wireless networks," *IEEE Access*, vol. 5, pp. 16693–16746, 2017.

[14] G. Kaddoum, M. F. A. Ahmed, and Y. Nijsure, "Code index modulation: A high data rate and energy efficient communication system," *IEEE Commun. Lett.*, vol. 19, no. 2, pp. 175–178, Feb. 2015.

[15] G. Kaddoum, Y. Nijsure, and H. Tran, "Generalized code index modulation technique for high-data-rate communication systems," *IEEE Trans. Veh. Technol.*, vol. 65, no. 9, pp. 7000–7009, Sep. 2016.

[16] W. Xu, T. Huang, and L. Wang, "Code-shifted differential chaos shift keying with code index modulation for high data rate transmission," *IEEE Trans. Commun.*, vol. 65, no. 10, pp. 4285–4294, Oct. 2017.

[17] W. Xu, L. Wang, and G. Kolumbán, "A novel differential chaos shift keying modulation scheme," *Int. J. Bifurcation Chaos*, vol. 21, no. 3, pp. 799–814, 2011.

[18] W. K. Xu, L. Wang, and G. Kolumbán, "A new data rate adaption communications scheme for code-shifted differential chaos shift keying modulation," *Int. J. Bifurcation Chaos*, vol. 22, no. 8, pp. 1–8, 2012.

[19] T. Huang, L. Wang, W. Xu, and F. C. M. Lau, "Multilevel code-shifted differential-chaos-shift-keying system," *IET Commun.*, vol. 10, no. 10, pp. 1189–1195, Jul. 2016.

[20] Y. Tan, W. Xu, T. Huang, and L. Wang, "A multilevel code shifted differential chaos shift keying scheme with code index modulation," *IEEE Trans. Circuits Syst., II, Exp. Briefs*, vol. 65, no. 11, pp. 1743–1747, Nov. 2018.

[21] G. Kaddoum, E. Soujeri, and Y. Nijsure, "Design of a short reference noncoherent chaos-based communication systems," *IEEE Trans. Commun.*, vol. 64, no. 2, pp. 680–689, Feb. 2016.

[22] W. Xu, Y. Tan, F. C. M. Lau, and G. Kolumbán, "Design and optimization of differential chaos shift keying scheme with code index modulation," *IEEE Trans. Commun.*, vol. 66, no. 5, pp. 1970–1980, May 2018.

[23] M. Herceg, D. Vranješ, G. Kaddoum, and E. Soujeri, "Commutation code index DCSK modulation technique for high-data-rate communication systems," *IEEE Trans. Circuits Syst., II, Exp. Briefs*, vol. 65, no. 12, pp. 1954–1958, Dec. 2018.

[24] M. Herceg, G. Kaddoum, D. Vranješ, and E. Soujeri, "Permutation index DCSK modulation technique for secure multiuser high-data-rate communication systems," *IEEE Trans. Veh. Technol.*, vol. 67, no. 4, pp. 2997–3011, Apr. 2018.

[25] G. Kaddoum, F.-D. Richardson, and F. Gagnon, "Design and analysis of a multi-carrier differential chaos shift keying communication system," *IEEE Trans. Commun.*, vol. 61, no. 8, pp. 3281–3291, Aug. 2013.

[26] G. Cheng, L. Wang, W. Xu, and G. Chen, "Carrier index differential chaos shift keying modulation," *IEEE Trans. Circuits Syst., II, Exp. Briefs*, vol. 64, no. 8, pp. 907–911, Aug. 2017.

[27] G. Cheng, L. Wang, Q. Chen, and G. Chen, "Design and performance analysis of generalised carrier index M-ary differential chaos shift keying modulation," *IET Commun.*, vol. 12, no. 11, pp. 1324–1331, Jun. 2018.

[28] W. Dai, H. Yang, Y. Song, and G. Jiang, "Two-layer carrier index modulation scheme based on differential chaos shift keying," *IEEE Access*, vol. 6, pp. 56433–56444, 2018.

[29] M. Miao, L. Wang, M. Katz, and W. Xu, "Hybrid modulation scheme combining PPM with differential chaos shift keying modulation," *IEEE Wireless Commun. Lett.*, vol. 8, no. 2, pp. 340–343, Apr. 2019.

[30] A. Papoulis, *Probability, Random Variables, and Stochastic Processes*. New York, NY, USA: McGraw-Hill, 1991.

[31] Y. Xia, C. Tse, and F. C. M. Lau, "Performance of differential chaos-shift-keying digital communication systems over a multipath fading channel with delay spread," *IEEE Trans. Circuits Syst., II, Exp. Briefs*, vol. 51, no. 12, pp. 680–684, Dec. 2004.

[32] J. G. Proakis and M. Salehi, *Digital Communications*. New York, NY, USA: McGraw-Hill, 2007.

[33] G. Kaddoum, P. Charge, and D. Roviras, "A generalized methodology for bit-error-rate prediction in correlation-based communication schemes using chaos," *IEEE Commun. Lett.*, vol. 13, no. 8, pp. 567–569, Aug. 2009.

Xiangming Cai received the B.Sc. degree in information engineering from the Guangdong University of Technology, Guangzhou, China, in 2017. He is currently pursuing the M.Sc. degree with the Department of Information and Communication Engineering, Xiamen University, China. His research interests include chaos-based digital communications and their applications to wireless communications.

Weikai Xu (S'10–M'12) received the B.Sc. degree in electronic engineering from Chongqing Three Gorges College, Chongqing, China, in 2000, the M.Sc. degree in communication and information system from the Chongqing University of Posts and Telecommunications, Chongqing, in 2003, and the Ph.D. degree in electronic circuit and system from the Xiamen University, Xiamen, China, in 2011. From 2003 to 2012, he was a Teaching Assistant and an Assistant Professor with the Department of Communication Engineering, Xiamen University, where he is currently an Associate Professor with the Department of Information and Communication Engineering. His research interests include chaotic communications, underwater acoustic communications, channel coding, cooperative communications, and ultra-wideband.

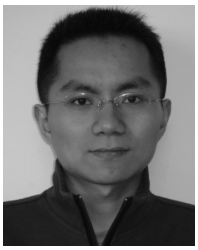

Shaohua Hong (M'12) received the B.Sc. degree in electronics and information engineering and the Ph.D. degree in electronics science and technology from Zhejiang University, Hangzhou, China, in 2005 and 2010, respectively. He is currently an Associate Professor with the Department of Information and Communication Engineering, Xiamen University, Xiamen, China. He is also an Associate Professor with the Shenzhen Research Institute, Xiamen University, Shenzhen, China. His research interests include joint source and channel coding, wireless communication, and image processing. He has been serving as an Editor for the *KSII Transactions on Internet and Information Systems* since 2015.

Lin Wang (S'99–M'03–SM'09) received the M.Sc. degree in applied mathematics from the Kunming University of Science and Technology, China, in 1988, and the Ph.D. degree in electronics engineering from the University of Electronic Science and Technology of China, China, in 2001. From 1984 to 1986, he was a Teaching Assistant with the Mathematics Department, Chongqing Normal University. From 1989 to 2002, he was a Teaching Assistant, a Lecturer, and an Associate Professor in applied mathematics and communication engineering with the Chongqing University of Posts and Telecommunications, China. From 1995 to 1996, he was with the Mathematics Department, University of New England, Armidale, NSW, Australia. In 2003, he was a Visiting Researcher with the Centre for Chaos and Complex Networks, Department of Electronic Engineering, City University of Hong Kong. In 2013, he was a Senior Visiting Researcher with the Department of Electronics and Communication Engineering, University of California at Davis, Davis, CA, USA. From 2003 to 2012, he was a Full Professor and the Associate Dean with the School of Information Science and Engineering, Xiamen University, China, where he has been a Distinguished Professor since 2012. He has authored over 100 journal and conference papers. He holds 14 patents in the field of physical layer in digital communications. His current research interests include channel coding, joint source and channel coding, chaos modulation, and their applications to wireless communication and storage systems.